Magnetism of HgSe:Fe

U. Zeitler,* A. Wittlin,† and J. C. Maan
High Field Magnet Laboratory, Research Institute for Materials, University of Nijmegen, 6525 ED Nijmegen, The Netherlands

W. Dobrowolski and A. Mycielski
Institute of Physics, Polish Academy of Science, Al. Lotników 32/46, 02-668 Warsaw, Poland
(Received 22 May 1996)

The perpendicular and parallel components of the magnetization of the mixed valence system $Hg_{1-x}Fe_xSe$ in the strongly dilute limit ($x<10^{-3}$) have been measured in magnetic fields up to 20 T. In this interesting semimagnetic semiconductor the overall magnetization is caused simultaneously by Fe^{3+} (Brillouin paramagnet), Fe^{2+} (van Vleck paramagnet), and free electrons (diamagnetic de Haas–van Alphen effect). Using a torque magnetometer the various contributions with their anisotropy are individually determined. For very low iron content ($x<2.4\times10^{-4}$) the Fe donors exclusively exhibit an isotropic Brillouin paramagnetism of noninteracting Fe^{3+} ions. For higher concentration Fe^{2+} also exists. Coexisting with the Brillouin paramagnetism of Fe^{3+} the Fe^{2+} reveal an induced van Vleck-type paramagnetism with a crystal-field-induced anisotropy. This anisotropy is analyzed by measuring the induced magnetic moment perpendicular to the magnetic field when applying the field in a nonsymmetric direction of the crystal. Using recent theoretical results on the energy-level diagram of Fe^{2+} in the T_d symmetry of a HgSe host lattice we deduce a spin-orbit level splitting of 2 meV from our experimental data. In contrast to higher concentration samples, both the Brillouin paramagnetism of Fe^{3+} and the van Vleck paramagnetism of Fe^{2+} can be attributed to the sum from individual Fe donors with no obvious magnetic interaction between them. Finally, we also have measured de Haas–van Alphen oscillations of the conduction-band electrons with amplitudes of the same order as the paramagnetic background. From the measured crystal-field-induced anisotropy in the magnetic moment we deduce a Fermi-surface anisotropy of about 7%. [S0163-1829(96)01945-5]

I. INTRODUCTION

In the semimagnetic semiconductor $Hg_{1-x}Fe_xSe$, a mixed valence system of Fe^{3+} and Fe^{2+},[1] the overall magnetization is caused simultaneously by the Brillouin paramagnetism of Fe^{3+}, the van Vleck paramagnetism of Fe^{2+}, and the diamagnetic de Haas–van Alphen (dHvA) effect of free electrons.[2] The magnetism of Fe^{2+} in HgSe and similar iron-based semimagnetic semiconductors has been studied intensively in recent years and analyzed in terms of a van Vleck-type paramagnetism with a crystal-field-induced anisotropy.[3–6]

However, apart from Fe^{2+} also a very small quantity of Fe^{3+} exists in the system. This is related to the fact that in the zero-gap system HgSe a resonant Fe^{2+} state is situated about 220 meV above the conduction-band edge.[1] Therefore, a small amount of Fe atoms loses an electron to the conduction band until the Fermi energy reaches the Fe^{2+} level. The remaining iron atoms will stay in the 2+ valence state, and the system forms a mixed valence system with both Fe^{2+} and Fe^{3+} present. If the Fe concentration is lower than a critical value $n_c\approx4.5\times10^{18}$ cm^{-3} (corresponding to an Fe content of $x\approx2.4\times10^{-4}$), the Fermi energy remains below the Fe^{2+} level and only ionized iron atoms in the 3+ valence state exist.

Apart from the paramagnetic background of the iron donors, dHvA oscillations occur in the magnetism of the system provided the electron mobility is high enough.[7] This contribution also reveals an anisotropic behavior due to a slight anisotropy of the Fermi surface in the zinc-blende host lattice. The number of electrons equals the number of Fe^{3+} impurities. Therefore, if only a few Landau levels are occupied (which is the case for magnetic fields exceeding 10 T), the dHvA amplitude is of the same order of magnitude as the Fe^{3+} saturation magnetization, namely, a few Bohr magnetons per electron.

In this work we perform an experimental analysis of the magnetic properties of iron donors in strongly diluted $Hg_{1-x}Fe_xSe$ and the dHvA effect of the free electrons. In Sec. II we will first describe the experimental procedure and explain how torque magnetometry can be used to measure accurately a small magnetization both parallel and perpendicular to the applied magnetic field. In Sec. III we will then introduce shortly into the theoretical background concerning the magnetism of Fe^{3+}, of Fe^{2+} in the crystal field of a HgSe host lattice and the dHvA effect of free electrons.

The experimental results are presented and analyzed in Sec. IV. For very low concentrations ($n_{Fe}<n_c$) we will show in Sec. IV A that the magnetism of the Fe donors can be described qualitatively as well as quantitatively by an isotropic Brillouin paramagnetism of noninteracting Fe^{3+} ions.

For higher concentrations an anisotropy begins to appear in the magnetization which is attributed to the crystal-field-induced anisotropy of a van Vleck-type paramagnetism of Fe^{2+} (Sec. IV B). Rather than looking at the magnetization parallel to the applied magnetic field we will use torque magnetometry to concentrate on the perpendicular magnetization which only occurs for an anisotropic system, i.e., for Fe^{2+}, but not for Fe^{3+}, and neither for the diamagnetism of the lattice. The results are interpreted in the framework of re-

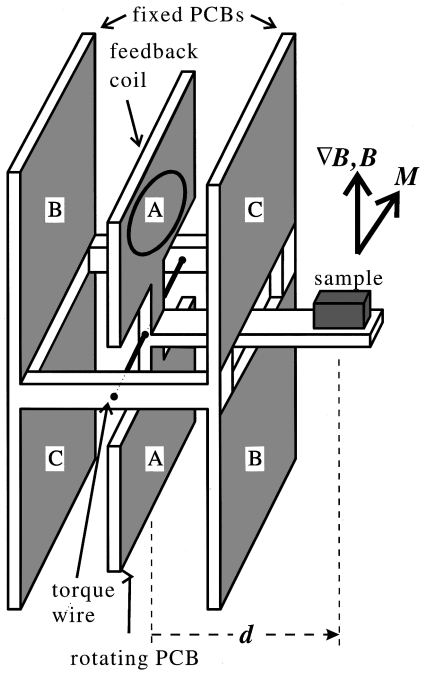

FIG. 1. Sketch of the torque magnetometer.

cently published theoretical work on the magnetic properties of Fe^{2+} in the T_d crystal field of a II-VI host lattice.[6]

Finally, we will investigate the anisotropy of the Fermi surface in Sec. IV C by looking at the perpendicular and parallel components of the oscillating contributions of the magnetization.

II. EXPERIMENT

The samples were grown using the Bridgeman method at the Polish Academy of Science. Subsequently they were oriented using standard Laue techniques and cut with a wire-erosion machine to parallelepipeds of about $3\times1.5\times1.5$ mm^3 with the faces oriented in the (100) direction. We measured samples with four different nominal iron concentrations $n_{Fe}=2.5$, 5, 7.5, and 10×10^{18} cm^{-3} both below and above the critical iron concentration for the existence of a mixed valence system.

To measure magnetization we used a highly sensitive torsional magnetometer[8] as sketched in Fig. 1. It consists of a rotating printed circuit board which is fixed on a 100 μm tungsten wire. Perpendicular to the wire axis an arm is mounted on which the sample is fixed in a distance $\vec{d}$ from the wire. A torque on the system will rotate the central board. The rotation angle φ with respect to the equilibrium position of the device is determined by measuring the change in the ratio of the capacitances C_{AB}/C_{AC} between the rotating inner electrode A and the fixed outer electrodes B and C.

A magnetization $\vec{M}$ of the sample will lead to a torque $\vec{T}$ on the device given by

$$\vec{T}=\vec{\nabla}(\vec{M}\cdot\vec{B})\times\vec{d}+\vec{M}\times\vec{B}. \tag{2.1}$$

The first term arises from the force $\vec{\nabla}(\vec{M}\cdot\vec{B})$ exerted on the sample if it is placed in a field gradient; the second one measures the component $M_\perp$ of the magnetization perpendicular to the applied magnetic field and to the torque axis. In our experiments the torque axis is perpendicular to the applied magnetic field.

The torque meter is calibrated by applying a current I through a feedback coil wound around the central electrode. This current produces a magnetic moment $M^{fb}=IA$ (A is the surface of the coil) perpendicular to the applied magnetic field which leads to a calibrated torque $T=M^{fb}B$ on the magnetometer.

Since the natural field gradient in a coil is proportional to the total field B, Eq. (2.1) can be rewritten in the form

$$T=B(\alpha M_\parallel+M_\perp), \tag{2.2}$$

where $M_\parallel$ is the component of $\vec{M}$ in the field direction and α is a geometric factor depending on the position of the sample in the coil and its distance d to the torque axis. Since α is in general small (of the order of a few percent), the torque meter is much more sensitive to a perpendicular magnetization $M_\perp$ arising from a magnetic anisotropy than to the isotropic contribution $M_\parallel$. In the case when either no field gradient is present or the sample is placed or the torque axis α equals zero. This configuration is generally used to measure the magnetic properties of highly anisotropic systems like two-dimensional electron gases,[9] organic conductors,[10] and high-T_c superconductors.[8] On the other hand, as described above, mounting the sample at a finite distance d from the torque axis and measuring T for two different positions of the torque meter (i.e., two different values of α) not only $M_\perp$ but also the isotropic contribution $M_\parallel$ can be obtained.

We have measured several HgSe:Fe samples in the magnetic field of a Bitter coil up to 20 T. The samples were placed in a distance of $d\approx5$ mm from the torque wire either close to the center of the magnetic field or in a vertical distance of about 5 cm from the center where an appreciable field gradient is present. These two positions correspond to $\alpha=0.002$ and $\alpha=0.033$, respectively. The absolute value of α can be determined within about 10%, the error mainly arising from the uncertainty in the distance d of the sample to the torque wire. This leads to the same uncertainty in the absolute calibration of the magnetization $M_\parallel$.

III. THEORETICAL BACKGROUND

The ground state of Fe^{3+} is a spin sextet $^6S_{5/2}$ with zero orbital momentum. The permanent magnetic moment leads to a Brillouin-type paramagnetic behavior. In that respect Fe^{3+} is isoelectronic to Mn^{2+} the properties of which in diluted magnetic semiconductors have been studied very extensively.[11] For low enough concentrations the Fe-Fe interactions can be neglected. Since the ground state of Fe^{3+} has no orbital momentum, no LS coupling exists and thus no crystal-field-induced anisotropy can occur. Therefore, the magnetization of Fe^{3+} in HgSe is described accurately as that of free Fe^{3+} ions which will be confirmed experimentally in Sec. IV A.

Fe^{2+} is more complicated, since the free-ion ground state $^5D_0$, with a vanishing magnetic moment, is split in the tetrahedal crystal field of the HgSe lattice into an orbital doublet $^5\Gamma_3$ and an orbital triplet $^5\Gamma_5$ situated an energy Δ

above ${}^5\Gamma_3$.[12] Due to the strong spin-orbit interaction $H_{SO}=\lambda\vec{L}\cdot\vec{S}$, ${}^5\Gamma_3$ splits into five equidistant levels Γ_1, Γ_4, Γ_3, Γ_5, and Γ_2 separated by $6\lambda^2/\Delta$. An applied magnetic field $\vec{B}$ removes the remaining degeneracy of these levels and ten individual energy levels are found. Since the energies of these levels have a different magnetic field dependence for different directions of the magnetic field, an anisotropy in the total magnetization is observed.[4–6]

In more general terms, in the T_d symmetry of a crystal the dependence of any scalar physical property x on the direction of the magnetic field $\vec{n}=\vec{B}/B$ can be expanded as a function of even powers of the components of $\vec{n}$ such that each term is invariant under the symmetry operations of the T_d symmetry:

$$x(B,\vec{n})=x_0(B)+\sum_{k=1}^{\infty} x_{2k}(B)f_{2k}(\vec{n}), \tag{3.1}$$

where $x_0(B)$ is field dependence of x if a magnetic field is applied in the [100] direction. In the T_d symmetry the first nonvanishing terms of the expansion are $f_4(\vec{n})=(n_x^2n_y^2+n_y^2n_z^2+n_z^2n_x^2)$ and $f_6(\vec{n})=(n_x^2n_y^2n_z^2)$.[13]

Applying this concept to the free energy $F(B,T)=-kT\ln\Sigma_i\exp[-\epsilon_i(B)/kT]$ we can calculate the magnetic moment $\vec{m}=-dF/d\vec{B}$ per Fe^{2+} atom. Here $\epsilon_i(B)$ are the individual energy states of a Fe^{2+} in a T_d environment calculated theoretically in Ref. 6. In principle, this can be done for any direction of an applied magnetic field up to an order $2k$ ($k\geqslant 2$) by calculating the energy levels ϵ_i for k discrete field directions. Restricting ourselves to the lowest nonvanishing orders the free energy can be written as

$$F(\vec{B},T)=F_0(B,T)+F_4(B,T)f_4(\vec{n})+F_6(B,T)f_6(\vec{n})\cdots. \tag{3.2}$$

The components of the magnetic moment per iron atom are given by

$$\begin{aligned} m_r &= -\frac{dF_0}{dB}-\frac{dF_4}{dB}f_4-\frac{dF_6}{dB}f_6-\cdots, \\ m_\vartheta &= -\frac{F_4}{B}\frac{df_4}{d\vartheta}-\frac{F_6}{B}\frac{df_6}{d\vartheta}-\cdots, \\ m_\varphi &= -\frac{F_4}{B\sin\vartheta}\frac{df_4}{d\varphi}-\frac{F_6}{B\sin\vartheta}\frac{df_6}{d\varphi}-\cdots, \end{aligned} \tag{3.3}$$

where (r,ϑ,φ) represent the direction of the magnetic field with respect to the [100] direction of the host lattice. Only for a field applied in a symmetry direction of the crystal will both the perpendicular components m_ϑ and m_φ vanish.

As can be seen in Eq. (3.3) the magnetic moment m_r parallel to the field is essentially given by $-dF_0/dB$. Since the crystal-field-induced angular-dependent modifications $F_4, F_6, \ldots$ are in general small with respect to F_0, only a small anisotropy in the parallel magnetization occurs.[4,5] In contrast, for a field applied in a nonsymmetry direction of the crystal, the first nonvanishing term in the magnetic moment perpendicular to the field is proportional to F_4/B and measures directly the anisotropy of the free energy.

Measuring torque in the absence of a field gradient therefore provides a quantity which only reflects the anisotropy, independent of the large background in the parallel magnetization, and is given by $\vec{T}=\vec{B}\times\vec{m}_\perp$. In the particular case with the torque axis perpendicular to the ϑ direction (as in our experiments) the torque per ion can be expressed as

$$t_\varphi=-F_4\frac{df_4}{d\vartheta}-F_6\frac{df_6}{d\vartheta}-\cdots. \tag{3.4}$$

Restricting ourselves to the first term we can calculate F_4 using the energy level scheme of Fe^{2+} in a T_d crystal field given in Ref. 6 by calculating the free energy $F_{[100]}$ for a magnetic field applied in the [100] direction and $F_{[111]}$ for a field applied in the [111] direction as $F_4=(F_{[111]}-F_{[100]})/3$.

As described in Sec. I the same number of Fe^{3+} and free electrons in the conduction band exist (neglecting electrons from other impurities and vacancies, of course). In a quantizing magnetic field the magnetization of these electrons will exhibit dHvA oscillations. The value and the direction of the oscillatory contribution to the magnetization can be written as[14]

$$\begin{aligned} \vec{M}=&-\frac{3}{2^{3/2}\pi}\frac{m}{m^*}n\mu_B\sqrt{\frac{B}{P}}\sum_{p=1}^{\infty}\frac{(-1)^p}{p^{3/2}}\frac{pX_T}{\sinh(pX_T)}e^{-pX_D} \\ &\times\cos(p\pi\nu)\sin\left[2\pi p\frac{P}{B}-\frac{\pi}{4}\right]\hat{m}, \end{aligned} \tag{3.5}$$

where

$$\hat{m}=\vec{n}_r+\frac{1}{P}\frac{dP}{d\vartheta}\vec{n}_\vartheta+\frac{1}{P\sin\vartheta}\frac{dP}{d\varphi}\vec{n}_\varphi.$$

The normalized vectors $\vec{n}_i$ again assign the direction of the magnetic field. The amplitudes are damped by temperature ($X_T=2\pi^2k_BT/\hbar\omega_c$) and level broadening ($X_D=2\pi^2k_BT_D/\hbar\omega_c$, where T_D is the Dingle temperature). The dHvA frequency P can be defined with the extremal cross section A_{ext} of the Fermi surface perpendicular to the magnetic fields by

$$P=\left(\frac{\hbar}{2\pi e}\right)A_{ext}. \tag{3.6}$$

For a spherical Fermi surface the extremal cross section is $A_{ext}=\pi k_F^2$ (k_F is the Fermi wave vector). With $k_F=(3\pi^2n_{el})^{1/3}$ for parabolic bands we can directly deduce the free-electron concentration n_{el} from the dHvA frequency.

The angular dependence $dF/F\Theta$ measures the Fermi surface anisotropy caused by a different dispersion in different crystal directions. This quantity can by determined directly by measuring the longitudinal and the transverse magnetization M_r and M_ϑ simultaneously. The resolution of such a method is given by the resolution of the ratio M_ϑ/M_r.

For metals, with a large Fermi-surface anisotropy ($M_\vartheta/M_r\approx 1$) this technique is widely used to perform dHvA analysis on M_ϑ.[14] But also for semiconductors with a rather small Fermi-surface anisotropy of the order of a few percent the strong sensitivity of the torque on M_ϑ allows one to see the Fermi-surface anisotropy directly by applying a magnetic

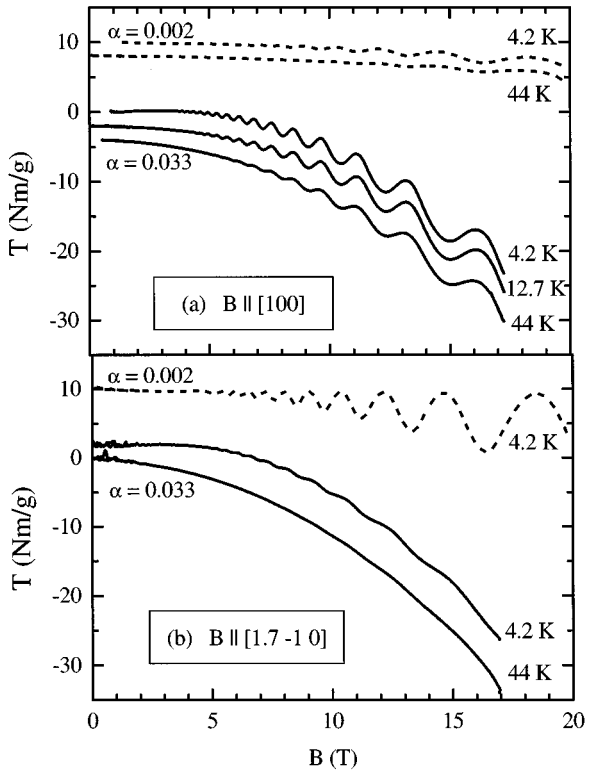

FIG. 2. The raw torque of sample A (nominal Fe concentration $n_{Fe} \approx 2.5\times10^{18}$ cm^{-3}) measured for $\alpha=0.033$ (solid lines) and $\alpha=0.002$ (dashed lines). In (a) the magnetic field is oriented along [100], in (b) along [1.7 −1 0].

field in a nonsymmetry direction of the crystal. This is in contrast to direct magnetization measurements[7] where the Fermi-surface anisotropy only can be deduced from distinct dHvA measurements with a magnetic field applied in different crystal directions.

IV. RESULTS AND DISCUSSION

A. Brillouin paramagnetism of Fe^{3+}

The experimentally measured torque for a sample with a very low Fe concentration (sample A, nominal iron concentration $n_{Fe}=2.5\times10^{18}$ cm^{-3}) is shown in Fig. 2. Three other samples (cut from the same mother piece) showed qualitatively as well as quantitatively the same results. In Fig. 2(a) the magnetic field has been oriented (within about 5°) in the (100) direction of the crystal and the torque axis along the (001) direction. In order to investigate anisotropy, we have rotated the sample from the [001] direction by −30° and performed the same set of experiments with the magnetic field applied in the [1.7 −1 0] direction; the torque was measured again along [001] [Fig. 2(b)]. In an anisotropic system, an additional torque is expected due to the magnetization $M_\perp$ for fields away from symmetry direction.

In the presence of a field gradient (solid lines, $\alpha=0.033$) the torque for both field orientations is dominated by a temperature-independent diamagnetic background, leading to a quadratic field dependence in the signal. The main part of this background arises from the diamagnetism of the HgSe lattice, a small part from the diamagnetic background of the magnetometer. This diamagnetic background is isotropic ($M_\perp^{diam}=0$ for both field directions) as seen from the independence of the signal on the direction of the applied magnetic field (oriented along a symmetry direction of the crystal or not) and from the almost negligible background in a much smaller gradient ($\alpha=0.002$, dashed line).

With a small field gradient ($\alpha=0.002$) the dominant part to the signal is the contribution from the dHvA oscillations arising from an anisotropic Fermi surface.[7] As expected, this anisotropic contribution $M_\perp^{dHvA}$ to the dHvA effect is small if the field is oriented close to a symmetry direction of the crystal [Fig. 2(a)] and is strongly enhanced if the magnetic field is not oriented in a symmetry direction [Fig. 2(b)]; see Sec. IV C for more details.

Removing the diamagnetic background and using Eq. (2.2) we can determine the magnetization $M_\parallel$ and $M_\perp$ of the sample which contains a paramagnetic background arising from the Fe donors and an oscillatory contribution arising from the dHvA effect of the electrons. The nonoscillatory part of the paramagnetic contribution to the torque is found not to depend on the orientation of the field and no perpendicular contribution $M_\perp^{para}$ exists for any field direction. This behavior is expected for the angular singlet ($L=0$) ground state of Fe^{3+} which forbids coupling of different eigenstates with the crystal field, thus leading to an isotropic magnetic field dependence. Therefore, the spin of 5/2 leads to a total magnetic moment of $J=5/2$. Like for Mn in a II-VI host lattice[11] Fe-Fe interactions are found to be totally negligible for the very low concentrations we are dealing with. The total magnetization is thus simply given by the sum of the magnetic moments of individual Fe^{3+} ions.

This statement is verified experimentally in Fig. 3 where we have plotted the magnetization $M_\parallel$ for $\vec{B} \parallel [100]$. The same results were obtained for other field directions and also for different samples with the same iron content. In the same figure the theoretically expected curves $ngJB_J(gJ\mu_B B/kT)$ are plotted. Here $B_J(x)$ are the Brillouin functions, n is the iron concentration, $J=5/2$ is the total momentum of a Fe^{3+} atom, $g=2$ is its g factor, and $\mu_B=9.27\times10^{-24}$ J/T is the Bohr magneton. The only fit parameter we used is the iron concentration which was found to be 3.0×10^{18} cm^{-3}. The experimentally measured saturation value corresponds to the theoretically expected value of $5\mu_B$ per atom. The discrepancy between the experimentally found Fe concentration and the nominal Fe content of 2.5×10^{18} cm^{-3} is due to a technological uncertainty of the precise content and to an uncertainty in the calibration of the magnetization axis (see Sec. II).

Independent from the magnetization due to the Fe^{3+} impurities we can determine the free-electron concentration using the dHvA effect. From a dHvA period of $F=70$ T we find $n_{el}=3.3\times10^{18}$ cm^{-3}, slightly higher than the iron concentration of $n_{Fe}=3.0\times10^{18}$ cm^{-3} determined from the saturation magnetization. Apart from the already above mentioned reasons this small discrepancy is also due a small Fermi-surface anisotropy and a nonparabolicity of the conduction band, leading to an error in the deduction of n_{el} from dHvA experiments. Moreover, free electrons may not only originate from Fe donors but also from Se vacancies in the host lattice.

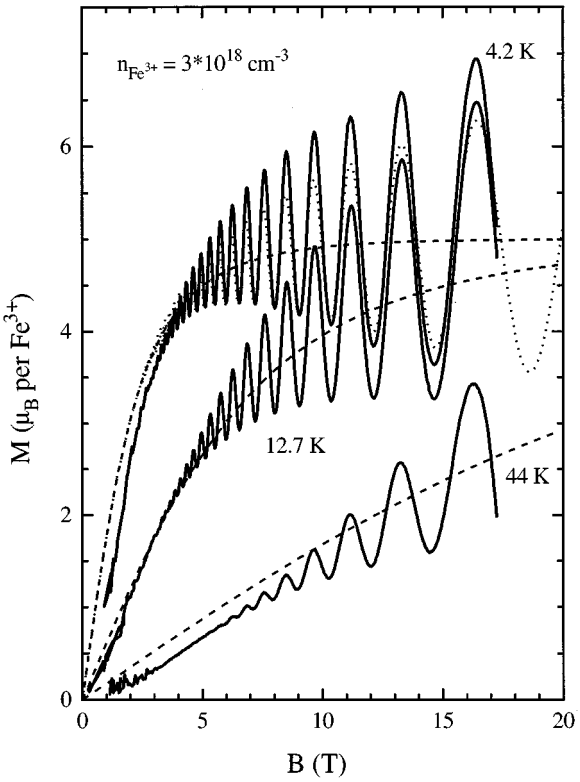

FIG. 3. The magnetization $M_{\parallel}$ of sample A ($x \approx 1.4\times10^{-4}$) for a magnetic field oriented in the [100] direction. The diamagnetic background of the lattice and of the magnetometer has been removed. The dashed lines represent the theoretically expected Brillouin paramagnetism of Fe^{3+} with an iron concentration of $n = 3\times10^{18}$ cm^{-3}. Superimposed in this paramagnetic background dHvA oscillations of free electrons are visible; see Sec. IV C. The dotted line shows a fit for the dHvA oscillations at 4.2 K, the only fit parameters being the Dingle temperature of 7 K and a free-electron concentration of $n_{el} = 3.3\times10^{18}$ cm^{-3}.

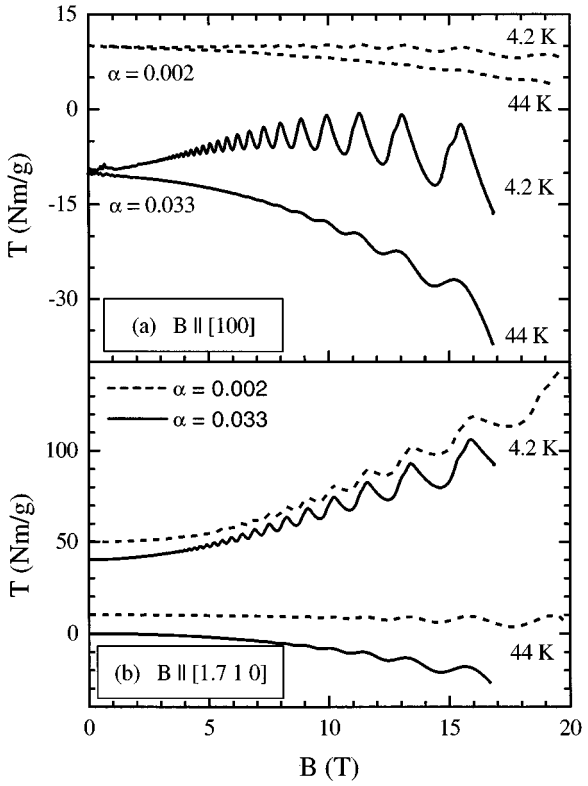

FIG. 4. The raw torque of sample B (nominal Fe concentration $n_{Fe} \approx 10\times10^{18}$ cm^{-3}) for $\alpha = 0.033$ (solid lines) and $\alpha = 0.002$ (dashed lines) with a magnetic field oriented along [100] (a) and along [1.7 1 0] (b).

B. Anisotropic van Vleck paramagnetism of Fe^{2+}

The magnetization of the Fe^{3+} described above is markedly different from the magnetism of Fe^{2+} in the T_d crystal-field environment of the HgSe lattice which is known to reveal a crystal-field-induced magnetic anisotropy at low temperatures. In Fig. 4 we show the experimental torque of sample B (nominal Fe concentration $n_{Fe} \approx 10\times10^{18}$ cm^{-3}) with a 4 times higher Fe content than sample A, and well above the critical concentration where a mixed valence system of Fe^{3+} and Fe^{2+} is expected.

For a field parallel to the symmetry direction [100] (within 5°) the torque is again essentially due to a diamagnetic background dominating at high temperatures and a paramagnetic contribution parallel to the field dominating for lower temperatures. (The diamagnetic background at $\alpha = 0.002$ and $T = 4.2$ K is mainly due to the intrinsic diamagnetism of the magnetometer.)

If the field is turned away by $\Theta = 30°$ from the [100] symmetry direction ($B \| [1.7\ 1\ 0]$), the situation changes drastically. At low temperatures, a torque appears which is essentially independent of the field gradient and which is also an order of magnitude larger than that due to a parallel magnetization visible in Fig. 4(a). This additional contribution is therefore caused by a magnetization *perpendicular* to the magnetic field and reflects solely the anisotropy of Fe^{2+}.

To visualize this we have plotted the perpendicular torque $T_{\perp}$ at 4.2 K only due to the perpendicular magnetization for four samples with different Fe concentrations ($n_{Fe} = 2.5$, 5, 7.5, and 10×10^{18} cm^{-3}) in Fig. 5; the diamagnetic background of the magnetometer has been removed. As described in Sec. II we can extract $T_{\perp}$ from $T_{\perp} = [\alpha_2 T(\alpha_1) - \alpha_1 T(\alpha_2)]/(\alpha_2 - \alpha_1)$, where $T(\alpha_i)$ is the experimentally measured total torque for $\alpha_1 = 0.002$ and $\alpha_2 = 0.033$, respectively. Since the total torque for $\alpha_1 = 0.002$ only differs by less than 2% from the perpendicular torque, the above extraction procedure for $T_{\perp}$ is very insensitive to uncertainties in α. We can therefore extrapolate the lines up to a maximal magnetic field of 20 T (as achieved when $\alpha = 0.002$) by extrapolating the results for $\alpha = 0.033$ to 20 T without making a relative error larger than the experimental uncertainties.

As shown in Fig. 5 a perpendicular magnetization begins to show up with increasing Fe concentration: For the lowest concentration (nominally $n_{Fe} = 2.5\times10^{18}$ cm^{-3}, experimentally deduced $n_{Fe} = 3\times10^{18}$ cm^{-3}; see Sec. IV A) no Fe^{2+} exists in the system and therefore no perpendicular magnetization occurs in the paramagnetic background. For higher Fe concentrations the torque and therefore the perpendicular magnetization is proportional to the Fe^{2+} concentration as shown in the inset of Fig. 5. Here the Fe^{2+} concentration has been deduced from the total Fe concentration reduced by the Fe^{3+} concentration, which is essentially independent of the total Fe concentration for concentrations $n_{Fe} \geqslant 5\times10^{18}$

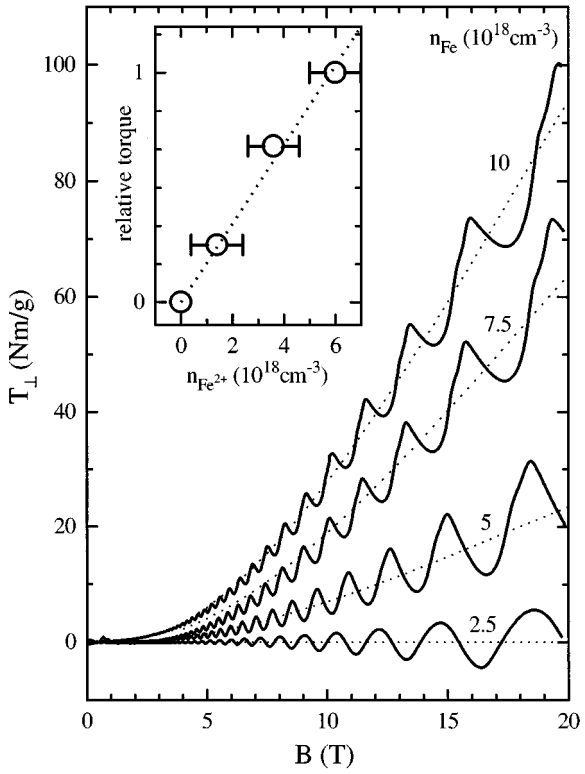

FIG. 5. The magnetic field dependence of the perpendicular torque at 4.2 K for four samples with different electron concentrations.

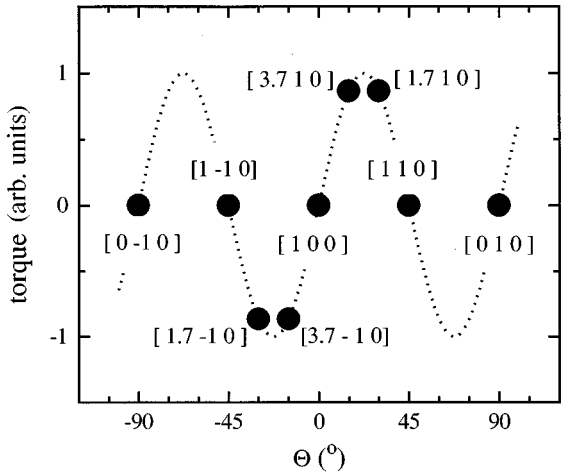

FIG. 6. The angular dependence of the perpendicular torque of Fe^{2+} along the [001] direction. ϑ indicates the angle between the magnetic field and the [100] direction for a rotation around the torque axis. The dotted line represents the expected behavior in a T_d crystal field; the points indicate angles where experiments have been performed.

cm^{-3}. As in Sec. IV A the Fe^{3+} concentration can be deduced experimentally from the free-electron concentration measured using the dHvA effect and an estimated contribution to the free-electron concentration from Se vacancies of $n_{vac} \approx 0.5 \times 10^{18}$ cm^{-3}. The error bars contain the uncertainty of the total concentration, an uncertainty in the estimation of Se vacancies, and an error in determining n_{el} from the dHvA effect.

We did also check whether the experimentally measured perpendicular torque depends on the direction of the magnetic field as expected in the T_d symmetry. To this end, several samples have been rotated from [100] around the [001] direction by $\Theta = -45°$, $-30°$, $-15°$, $0°$, $15°$, $30°$, and $45°$. Here the orientation of the torque axis is defined in a way that a positive perpendicular torque reflects a perpendicular magnetic moment which tends to decrease the above-defined angle Θ.

In the T_d symmetry, in the lowest nonvanishing order, the torque induced by a perpendicular magnetic moment is proportional to $df_4/d\Theta \propto \sin 4\Theta$, which is confirmed experimentally and shown in Fig. 6. As expected, within the experimental uncertainty for $\Theta(\pm 5°)$ the torque is the same for $\vartheta = 15°$ and $\vartheta = 30°$ and changes sign for $\vartheta = -15°$ and $\vartheta = -30°$. As already stated above, if the field is applied in a symmetry direction [100] or [110], no perpendicular torque occurs. The sign of the observed torque indicates that the sample always tends to turn in the direction of the closest [100] axis where the free energy is minimized already, showing qualitatively that the first anisotropic term in the free energy F_4 is positive as expected by theory.[6]

The fundamental reasons for the occurrence of a perpendicular magnetization are due to the crystal-field-induced anisotropy of the total free energy of a Fe^{2+} donor caused by an anisotropy in each individual energy level. In particular the perpendicular moment at low temperature reflects the anisotropy in the magnetic field dependence of the ground-state energy (if only terms up to F_4 are considered). Summing up all individual anisotropy contributions from each energy level (without thermal weighting) yields naturally a total zero anisotropy. Therefore, the perpendicular torque disappears if the temperature is much higher than the spacing between individual energy levels.[6]

Figure 7 shows that indeed the experimentally measured torque due to a perpendicular magnetization starts disappearing between 5 K and 20 K. In the inset we also show the theoretically expected temperature dependence of the torque with a level splitting $6\lambda^2/\Delta = 2$ meV which we used as a fit parameter. We have only taken into account the anisotropy due to the admixture of the ten energy levels of the $^5\Gamma_3$ level as calculated in Ref. 6. For low fields the experimental temperature dependence of the perpendicular magnetization is well reproduced by this simple model; for higher fields deviations occurs. These deviations are to be expected since the preceding analysis only considered the first nonvanishing corrections in the free energy. This becomes less justified at higher magnetic fields where the perpendicular magnetization contains considerable contributions of these higher-orders terms and a more sophisticated analysis has to be performed. In particular the precise energy-level structure of the system has to be known for more than two specific directions.

These unknowns make it not possible to extract the level splitting solely from the magnetic field dependence of the perpendicular magnetization. Of course it may be possible to obtain this information experimentally but only with a more accurate calibration of the direction of the magnetic field and

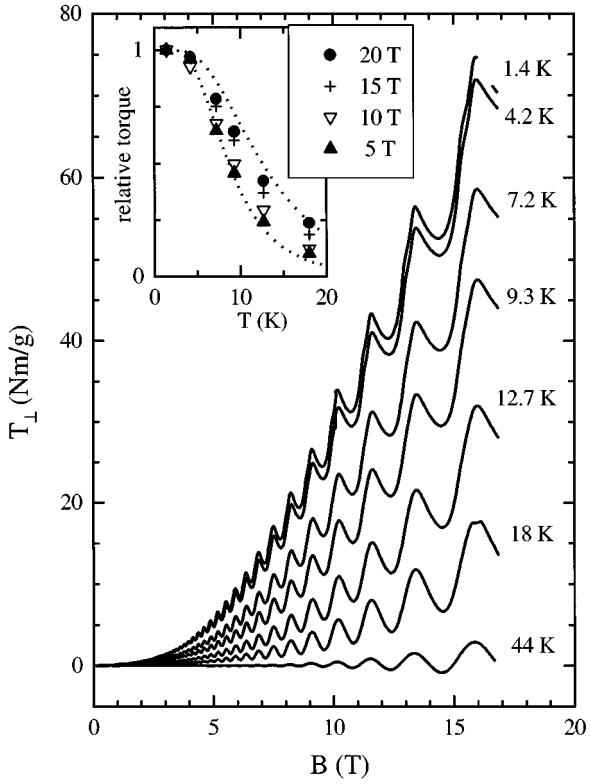

FIG. 7. The magnetic field dependence of the perpendicular torque of sample B for different temperatures. The inset shows the temperature dependence of the relative perpendicular torque of at different magnetic fields; the dashed lines represent the theoretically expected temperature dependence at 5 T and 20 T for a level splitting of 2 meV.

the torque axis with respect to the crystal directions. This might be done by performing angular dependent torque magnetometry.

However, even with very accurate experimental results, serious complications in the extraction of characteristic values for the energy level diagram of Fe^2 in HgSe arise from the influence of 15 higher states of the $^5\Gamma_5$ level. Since the separation Δ of $^5\Gamma_5$ from $^5\Gamma_3$ is orders of magnitude higher than the level splitting of the individual levels within $^5\Gamma_3$, their contribution to the free energy can of course totally be neglected. However, they have been shown to mix strongly to the ten levels of $^5\Gamma_3$ and to modify considerably the magnetic field dependence of these ten lowest levels.[6] These corrections become important when the magnetic-field-dependent corrections to the individual energy levels become comparable to the level splitting which occurs at fields higher than about 10 T.[6]

Finally, the strong field dependence of the torque due to a perpendicular magnetic moment ($\propto B^4$ for low fields) also shows unambiguously that the anisotropy in the magnetic moment is in fact an induced one which only becomes important in magnetic fields where the Zeeman splitting and the spin-orbit level splitting are of the same order. It occurs if a magnetic field induces a magnetic moment (van Vleck paramagnetism) and the mixing of the magnetic Zeeman term and the spin-orbit splitting causes a crystal-field-induced anisotropy.

C. de Haas–van Alphen oscillations of the conduction band electrons

Apart from the paramagnetic background the magnetization of sample A in Fig. 3 also contains an oscillating contribution due to the dHvA effect of free electrons. Similar oscillations are also observed in all the other samples. A first remarkable fact is the experimental accuracy of our method. In a first approximation, neglecting for a small Fermi-surface anisotropy, we can deduce the free-electron concentration from the dHvA period $F=70$ T to be $n=3.3\times10^{-18}$ cm^{-3}; the magnetic field dependence of the dHvA amplitudes yields a Dingle temperature of 7 K.

The theoretical fit not only reproduces the period and the field dependence of the oscillations used for the fit, but independently also their amplitude. The amplitude is given by the number of electrons present in the system. Compared to free electrons it is enhanced by a factor of m/m^* where m is the free-electron mass and $m^*=0.064m$ is the effective mass of the band electrons; see Eq. (3.5).

For samples with increasing iron concentration both amplitude and period first increase and then saturate in line with an increasing electron concentration saturating at 4.2×10^{18} cm^{-3}.

As for the magnetization of Fe^{2+} a perpendicular torque appears in the dHvA oscillations with the same angular dependence as for Fe^{2+} following the T_d symmetry of the HgSe host lattice. Therefore, this effect is again due to a crystal-field-induced anisotropy, in the case of band electrons an anisotropy in the dispersion relation leading to a Fermi-surface anisotropy.

Coincidentally, the perpendicular torque nearly exactly compensates the parallel contribution for a magnetic field in the $[1.7\ \ -1\ \ 0]$ direction and $\alpha=0.033$; see Fig. 2(b). This is the case for all the samples investigated. Therefore for this field direction we have $M_\perp\approx0.033M_\parallel$ for the oscillating dHvA contribution to the total magnetic moment.

Since the anisotropy follows the symmetry of the host lattice we can write in line with Eq. 3.1 in the lowest order $P(\vec{B})=P_0+P_4f_4(\vec{n})+\cdots$ for the extremal cross section of the Fermi surface with $P_4\approx0.07\times P_0$; i.e., we can deduce a maximal anisotropy in the dHvA period of about 7%. Of course these statements do not give a precise quantitative description of the Fermi surface of the system concerned but clearly explain the results qualitatively.

V. CONCLUSIONS

In conclusion we have performed a systematic study of the magnetic properties of Fe-doped HgSe. To extract a small anisotropic contribution we have used a torque magnetometer with a high sensitivity to magnetic moments perpendicular to the magnetic field but also the possibility to measure a small parallel magnetization accurately.

We have shown that the iron donors exist in two valence states: Fe^{3+} which reveals a perfect isotropic Brillouin paramagnetism of noninteracting atoms and Fe^{2+} with an anisotropic-induced van Vleck paramagnetism. A comparison of the experimental results concerning the anisotropy of the magnetization of Fe^{2+} with the theoretical energy-level diagram has been performed. In particular we could extract

an energy-level splitting of 2 meV of the five lowest-energy states; the complexity of the energy-level structure prevents us from extracting more quantitative parameters with confidence. Due to the very low electron concentration and the high sensitivity of the torque magnetometer, we were also able to measure dHvA oscillations of the free electrons where we could observe a small Fermi-surface anisotropy.

ACKNOWLEDGMENTS

We would like to thank L. W. M. Schreurs for his help with sample preparation. Part of this work was supported by the Stichting Fundamenteel Onderzoek der Materie which in turn is financially supported by NWO, and by the European Commission under Contracts Nos. CHRX-CT92-0062 and CHGT-CT-0051.

*Present address: Department of Physics, University of Nottingham, Nottingham NG7 2RD, UK. Electronic address: Ulrich.Zeitler@nottingham.ac.uk

†Present address: Institute of Physics, Polish Academy of Science, Al. Lotników 32/46, 02-668 Warsaw, Poland.

[1] A. Mycielski, P. Dzwonkowski, B. Kowalski, B.A. Orlowski, M. Dobrowolska, M. Arciszewska, W. Dobrowolski, and J.M. Baranowski, J. Phys. C **19**, 3605 (1986).

[2] K. Dybko, A. Lusakowski, J. Kossut, A. Arciszewska, P.J.E.M. van der Linden, A. Wittlin, J.A.A.J. Peerenboom, and A. Mycielski, Acta Phys. Pol. A **87**, 193 (1995).

[3] A. Twardowski, J. Appl. Phys. **67**, 5108 (1990).

[4] C. Testelin, C. Rigaux, A. Mauger, A. Mycielski, and M. Guillot, Phys. Rev. B **46**, 2193 (1992).

[5] Z. Wilamowski, H. Przybylinska, W. Joss, and M. Guillot, Semicond. Sci. Technol. **8**, S44 (1993).

[6] M. Villeret, S. Rodriguez, and E. Kartheuser, Phys. Rev. B **43**, 3443 (1991); see also E. Kartheuser, S. Rodriguez, and M. Villeret, *ibid.* **48**, 14 127 (1993) and references therein.

[7] M.M. Miller and R. Reifenberger, Phys. Rev. B **38**, 3423 (1988); **38**, 4120 (1988).

[8] J.C. Martinez, P.J.E.M. van der Linden, L.N. Bulaevskii, S. Brungersma, A. Koshlev, J.A.A.J. Perenboom, A.A. Menovsky, and P.H. Kes, Phys. Rev. Lett. **72**, 3614 (1994).

[9] J.P. Eisenstein, Appl. Phys. Lett. **46**, 635 (1985).

[10] P. Christ, W. Biberacher, H. Müller, and K. Andres, Solid State Commun. **91**, 451 (1994).

[11] S. Oseroff and P.H. Keesom, in *Diluted Magnetic Semiconductors*, Semiconductor and Semimetals, Vol. 25, edited by J.K. Furdyna and J. Kossut (Academic Press, Boston, 1988).

[12] We follow the group theoretical notation used in Ref. 6.

[13] The normalization factor of the functions $f^{(n)}$ has been chosen to be unity for further convenience.

[14] D. Shoenberg, *Magnetic Oscillations in Metals* (Cambridge University Press, Cambridge, England, 1984).